

ARTICLE

Received 17 Oct 2014 | Accepted 29 Jan 2015 | Published 10 Mar 2015

DOI: 10.1038/ncomms7444

Beating beats mixing in heterodyne detection schemes

G.J. Verbiest¹ & M.J. Rost²

Heterodyne detection schemes are widely used to detect and analyse high-frequency signals, which are unmeasurable with conventional techniques. It is the general conception that the heterodyne signal is generated only by mixing and that beating can be fully neglected, as it is a linear effect that, therefore, cannot produce a heterodyne signal. Deriving a general analytical theory, we show, in contrast, that both beating and mixing are crucial to explain the heterodyne signal generation. Beating even dominates the heterodyne signal, if the nonlinearity of the mixing element (mixer) is of higher order than quadratic. The specific characteristic of the mixer determines its sensitivity for beating. We confirm our results with both a full numerical simulation and an experiment using heterodyne force microscopy, which represents a model system with a highly non-quadratic mixer. As quadratic mixers are the exception, many results of previously reported heterodyne measurements may need to be reconsidered.

¹JARA-FIT and II. Institute of Physics, RWTH Aachen University, 52074 Aachen, Germany. ²Huygens-Kamerlingh Onnes Laboratory, Leiden University, Niels Bohrweg 2, 2333 CA Leiden, The Netherlands. Correspondence and requests for materials should be addressed to G.J.V. (email: Verbiest@physik.rwth-aachen.de) or to M.J.R. (email: Rost@physics.leidenuniv.nl).

There are many periodic processes with such a high frequency that they are difficult to measure experimentally. A solution is the application of a heterodyne detection scheme, as it down-converts the high-frequency signal to a lower, easily measurable frequency by mixing it with a reference signal. This enables the quantification of the amplitude, the phase and the frequency modulation of the original, high-frequency signal. A well-known example of a heterodyne detector is the radio. Heterodyne detection is also widely used in optics, in quantum devices, in the detection of nuclear magnetic resonance, in microwave detection, in scanning tunnelling spectroscopy and even in the search for gravitational waves^{1–7}.

Despite the successful application of heterodyne detection schemes, the exact generation of the heterodyne signal is often not well understood such that quantitative interpretations are only possible with extensive numerical calculations. Moreover, until now it has not been realized that the standard textbook equation for mixing usually fails, as in reality almost all mixers contain a beating stage at their input. To address this problem, we derived a general analytical theory that uses beating plus mixing for the generation of the heterodyne signal such that it becomes valid for all heterodyne detection schemes.

Although not recognized, almost all heterodyne mixers have a single input channel, through which a superposition is realized of the high-frequency signal and the reference signal before the real nonlinear mixing takes place: in optics, for example, the measured intensity is the square of the superposed electric fields. Consequently, we have to differentiate between beating, which is a linear effect occurring for superpositions and mixing occurring for nonlinear couplings.

In the following, we show that both beating and mixing are necessary to correctly describe the generation of the heterodyne signal. By deriving a general analytic theory that we confirm with simulations and experiments, we demonstrate that beating plays a crucial role in any type of heterodyne measurement system. In particular, we show that beating dominates mixing, if the mixer is of higher order than quadratic.

Results

Differentiating between Beating and Mixing. The upper panel of Fig. 1 depicts beating: it is the sum of two harmonic excitations at frequencies ω_s and ω_t . The result (black line) oscillates with a frequency ω_h ($\omega_s < \omega_h < \omega_t$) and beats in amplitude at the difference frequency $\omega_{\text{diff}} = |\omega_s - \omega_t|$ (red lines). However, as the Fourier transform of the time trace only shows the two original frequencies ω_s and ω_t , no signal is generated at the difference frequency ω_{diff} . Mixing, see lower panel of Fig. 1, is the product of two or more harmonic excitations and occurs if the transfer function of the mixer is of quadratic or higher order. This result really oscillates at the difference frequency (red line) and the sum frequency (black line). In contrast to beating, the Fourier transform shows the difference and the sum frequency, but not the two frequencies of the original harmonic excitations. Although beating and mixing are two intrinsically different effects that are classified by the type of mixer and their Fourier analyses, we will fully counterintuitively demonstrate that beating even dominates mixing, if the mixer is of higher order than quadratic!

To illustrate the importance of beating in heterodyne measurements, we use the example of heterodyne force microscopy (HFM)^{8–10}, as it represents a model system with a highly nonlinear mixing element (much higher order than quadratic). HFM enables the non-destructive imaging below a surface with nanometre resolution using an atomic force microscope^{11–19}. The typical excitation scheme is sketched in Fig. 2a. The subsurface information is contained in an ultrasonic sound wave that travelled through the sample with a frequency ω_s of several MHz

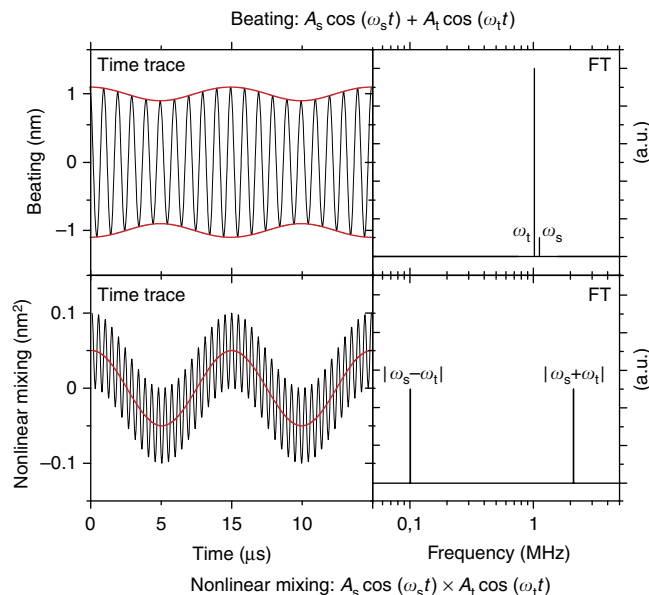


Figure 1 | Beating versus mixing. Beating is the sum of two harmonic functions (upper panel): the Fourier transform (FT) contains only the two original frequencies ω_s and ω_t . Mixing is the product of two harmonic functions (lower panel): the FT contains only the two nonlinear frequencies $|\omega_s - \omega_t|$ and $|\omega_s + \omega_t|$. The graphs have been calculated for $\omega_s = 1.1$ MHz, $\omega_t = 1$ MHz, $A_s = 0.1$ nm and $A_t = 1$ nm.

(well above the first resonance of the cantilever). To detect this signal, one applies a heterodyne detection scheme and excites, therefore, also the cantilever/tip with a high frequency ω_t that deviates slightly from ω_s . The nonlinear tip-sample interaction generates a heterodyne signal at a sufficiently low difference frequency ω_{diff} such that the cantilever really starts to move at ω_{diff} . In this way, the tip-sample distance is the superposition of the sample vibration with amplitude A_s and phase ϕ_s , and the cantilever vibration with amplitude A_t and phase ϕ_t , on the basis of which the nonlinear tip-sample interaction generates the difference frequency. Usually, one tunes ω_{diff} below the first resonance of the cantilever, however, this choice is not necessary, as long as the difference frequency can still excite a real motion in the cantilever. This information is provided by the transfer function of the cantilever, as it describes the reaction of the cantilever for a given applied force as a function of the frequency.

Figure 2b depicts the heterodyne signal generation for the example of HFM. The sum of the ultrasound signals at frequencies ω_t and ω_s results in beating at the mixer's input. This mixer generates a heterodyne drive force at ω_{diff} , which results in a real motion of the cantilever via the cantilever's transfer function $H(\omega_{\text{diff}})$. HFM is special, as the output of this transfer function (real motion at ω_{diff}) is coupled back into the tip-sample distance, which leads to an additional beating term at the input of the mixer. The transfer function also acts as a filter, which eliminates almost any contribution from the sum frequency $|\omega_t + \omega_s|$, as well as higher-order mixing terms: $A_{|\omega_s + \omega_t|}/A_{|\omega_s + \omega_t|} = 0.004$. We derive the transfer function in Supplementary Note 5.

We also address the general case without back coupling to the mixer below, as well as in Supplementary Note 4, and show that beating still gives significant corrections to the heterodyne signal. Although the back coupling can, in principle, also alter the ultrasonic amplitudes A_t and A_s (and corresponding phases), it was surprisingly shown experimentally that A_t and A_s remain constant for all tip-sample distances z in HFM^{20,21}. Therefore,

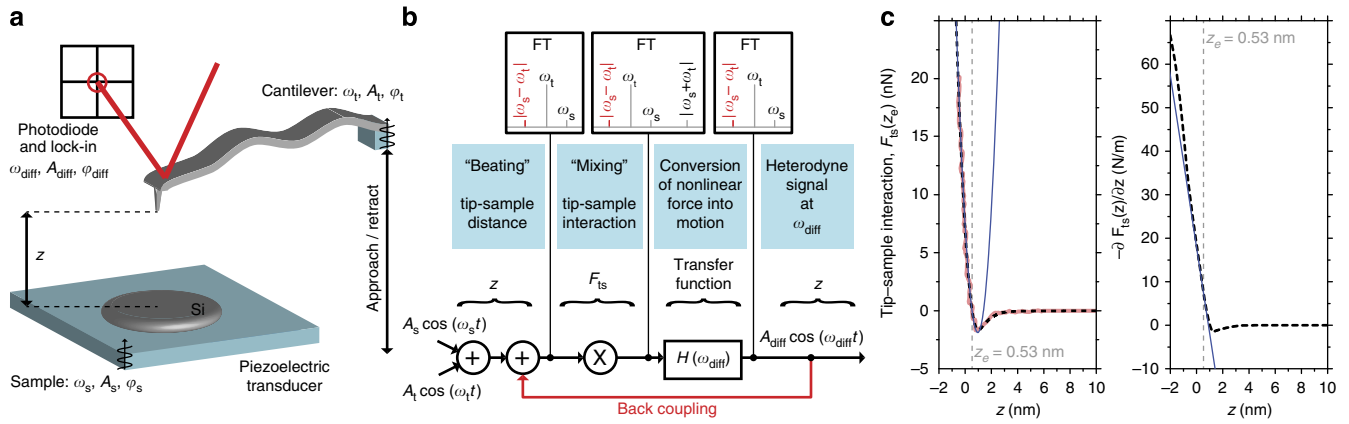


Figure 2 | Heterodyne force microscopy excitation scheme. (a) The Si sample vibrates with amplitude A_s and phase φ_s at a frequency ω_s , while the tip vibrates with A_t and φ_t at ω_t . Using an optical beam method and a lock-in, we detected the amplitude A_{diff} and phase φ_{diff} of the difference frequency $\omega_{diff} = |\omega_s - \omega_t|$. The tip-sample distance z was varied by moving the cantilever towards the surface (approach) and out again (retract). (b) The tip-sample distance is the sum of the ultrasonic motion of the cantilever $A_t \cos(\omega_t t)$ and the sample $A_s \cos(\omega_s t)$, which results in beating. The nonlinear tip-sample interaction generates drive forces (among others at the difference frequency), which lead, via the transfer function $H(\omega_{diff})$ of the cantilever that also acts as a low-pass filter, to a real motion that is coupled back into the tip-sample distance (red arrow). (c) The tip-sample interaction as a function of the distance z (left panel): obtained from the experiment (red), as used in the analytical calculation (dashed black), and a second-order approximation around $z_e = 0.53$ (blue). The derivative of the tip-sample interaction as a function of the distance z (right panel): as used in the analytical calculation (dashed black) and the second-order approximation around $z_e = 0.53$ (blue). The blue line is only a good approximation of F_{ts} near $z = z_e = 0.53$.

Table 1 | Analytical expressions for the heterodyne signal.

$A_{diff} e^{i\varphi_{diff}} = \frac{A_s A_t}{\sqrt{A_s^2 + A_t^2}} \frac{l_2 e^{i(\varphi_s - \varphi_t)}}{ H^{-1}(\omega_{diff}) e^{l_1 A} - l_1} \quad (2)$	
$\delta = l_0 / k \quad (3)$	
Standard Mixing	Beating & Mixing
$l_0 = F_{ts}(z_b + \delta)$	$l_0 = \frac{1}{\pi} \int_{-1}^1 F_{ts} \left(z_b + \delta + \sqrt{A_s^2 + A_t^2} u \right) \frac{du}{\sqrt{1-u^2}}$
$l_1 = \frac{\partial F_{ts}}{\partial z} (z_b + \delta)$	$l_1 = \frac{1}{\pi} \int_{-1}^1 \frac{\partial F_{ts}}{\partial z} \left(z_b + \delta + \sqrt{A_s^2 + A_t^2} u \right) \frac{du}{\sqrt{1-u^2}}$
$l_2 = \frac{1}{2} \sqrt{A_s^2 + A_t^2} \frac{\partial^2 F_{ts}}{\partial z^2} (z_b + \delta)$	$l_2 = \frac{1}{\pi} \int_{-1}^1 \frac{\partial F_{ts}}{\partial z} \left(z_b + \delta + \sqrt{A_s^2 + A_t^2} u \right) \frac{udu}{\sqrt{1-u^2}}$ $= \frac{\sqrt{A_s^2 + A_t^2}}{2\pi} \int_{-1}^1 \frac{\partial^2 F_{ts}}{\partial z^2} \left(z_b + \delta + \sqrt{A_s^2 + A_t^2} u \right) \sqrt{1-u^2} du$
<p>The general solutions (see Supplementary Notes 2 and 3) for the generated heterodyne signal (equation (2)), which is characterized by l_1 and l_2, and the static deflection (equation (3)), which is characterized by l_0. The parameters for 'Standard Mixing' are given in the first column, and for 'Beating & Mixing' in the second column. If one assumes a purely quadratic tip-sample interaction F_{ts}, the parameters of both solutions become equal. 'Beating & Mixing' explicitly takes into account the high-frequency motion and, therefore, the values of F_{ts} and $\partial F_{ts} / \partial z$ at all tip-sample distances between z_e and $z_e \pm A_h$.</p>	

HFM behaves exactly as a conventional heterodyne detection scheme with an additional back coupling of only the difference frequency signal $\omega_{diff} = |\omega_s - \omega_t|$ to the input of the mixer.

Analytical theory for the heterodyne signal generation. To derive an expression for the heterodyne signal, we need a description of the mixer's input, which is given by the tip-sample distance z . This distance contains a static offset z_b given by the position of the cantilever's base, a deflection δ and a back coupling term that accounts for the real motion at the difference frequency, in addition to the ultrasonic motion of both the cantilever and the sample.

$$z = z_b + \delta + A_{diff} \cos(\omega_{diff} t + \varphi_{diff}) + A_s \cos(\omega_s t + \varphi_s) + A_t \cos(\omega_t t + \varphi_t) \quad (1)$$

To enable a proper comparison between our theory and both a numeric simulation and experiments, we subtract an offset in z_b such that $z_b = 0$, if the deflection $\delta = 0$ during the approach cycle of the cantilever to the surface. Equation (1) is used for the input signal of the mixer, which generates via the nonlinear tip-sample interaction $F_{ts}(z)$ an effective drive force on the cantilever at the difference frequency. The derivation can be performed in two ways: either one makes, as usual, a second-order Taylor expansion of the tip-sample interaction around the equilibrium position (which is $z_e = z_b + \delta$) or one first uses beating to rewrite the high-frequency components of the mixer's input as a motion at a high frequency ω_h with amplitude $A_h = \sqrt{A_s^2 + A_t^2}$ and an additional amplitude modulated term at the same frequency, before making a linear expansion of the tip-sample interaction around a time varying equilibrium position. This linear expansion is justified, as a third-order expansion alters the heterodyne signal

at most by 4.5%. The first method, referred to as ‘Standard Mixing’ can be found in most textbooks, but (commonly not mentioned) this solution is valid only for second-order (quadratic) interactions. In contrast, our alternative approach, which we call ‘Beating & Mixing’, is valid for any type of interaction. The derivations and validities of both methods are described in detail in Supplementary Notes 2–4. ‘Beating & Mixing’ is a generalization of the standard theory and produces the ‘Standard Mixing’ results, if one artificially sets the beating term to zero. We find proof for our ‘Beating & Mixing’ description from excellent agreements of our results from numerical simulations and HFM experiments, as discussed below.

Let us now compare the ‘Standard Mixing’ textbook solution with our ‘Beating & Mixing’ generalization, in which the amplitude A_{diff} and the phase φ_{diff} of the heterodyne signal (Table 1; equation (2)) and the static deflection δ of the cantilever (Table 1; equation (3)) are determined by three parameters: I_0 denotes the average tip–sample interaction, I_1 denotes an effective tip–sample spring and I_2 represents the nonlinear characteristics (curvature) of the mixer. In the ‘Standard Mixing’ solution, I_1 and I_2 are determined by the values of the first and the second derivative of the tip–sample interaction at the equilibrium position z_e . In contrast, the ‘Beating & Mixing’ solution takes explicitly into account the high-frequency motion and, therefore, the derivative of the tip–sample interaction at all tip–sample distances between z_e and $z_e \pm A_h$. This description holds as long as $A_s \cdot A_t$ is smaller than A_h^2 . The three parameters I_0 , I_1 and I_2 become weighted integrals of F_{ts} and $\partial F_{\text{ts}}/\partial z$. Only if the mixer is purely quadratic, the integrals reduce to the exact values for I_0 , I_1 and I_2 of the textbook solution of ‘Standard Mixing’ (see Supplementary Note 3). Consequently, the ‘Beating & Mixing’ solution is required for all mixers that cannot be approximated with a quadratic function.

The tip–sample interaction in HFM deviates significantly from a quadratic behaviour. This becomes evident from the left panel of Fig. 2c, in which we show F_{ts} obtained from the experiment (red), F_{ts} as used in the analytical calculation (dashed black) and the quadratic interaction or second-order approximation of F_{ts} around $z = z_e = 0.53$ nm (blue). Although the quadratic interaction is a good approximation of the tip–sample interaction close to $z_e = 0.53$ nm, this approximation clearly fails 1 nm further at a tip–sample distance of, for example, $z = z_e = 1.53$ nm. This is even worse for the first derivative of the tip–sample interaction, which is shown in the right panel of Fig. 2c. Therefore, ‘Standard Mixing’ cannot describe the heterodyne signal generation in HFM: the tip–sample interaction cannot be approximated quadratically over a z range that is equal to the typical ultrasonic vibration amplitude A_h of 1 nm.

Experimental verification of the ‘Beating & Mixing’ theory.

In Fig. 3, we compare the ‘Beating & Mixing’ result with a full numerical simulation, an experiment, and the ‘Standard Mixing’ theory. For simplicity, we only show the approach curves. Both the ‘Beating & Mixing’ theory and the ‘Standard Mixing’ theory, as well as the numerical simulation, need an analytical description of the tip–sample interaction, which we obtained by fitting the Derjaguin–Muller–Toporov model²² and I_0 to the experimental deflection δ (see Supplementary Note 6). This experiment was performed with a 2 N m^{-1} cantilever, which had its first resonance frequency around 73 kHz. The sample was a freshly cleaned silicon wafer. The cantilever was excited at 2.87 MHz with an amplitude of 0.96 nm, while the sample was excited such that $\omega_{\text{diff}} = 1$ kHz. The vibration amplitude of the sample was 0.32 nm. The full experimental details are described in Supplementary Note 7.

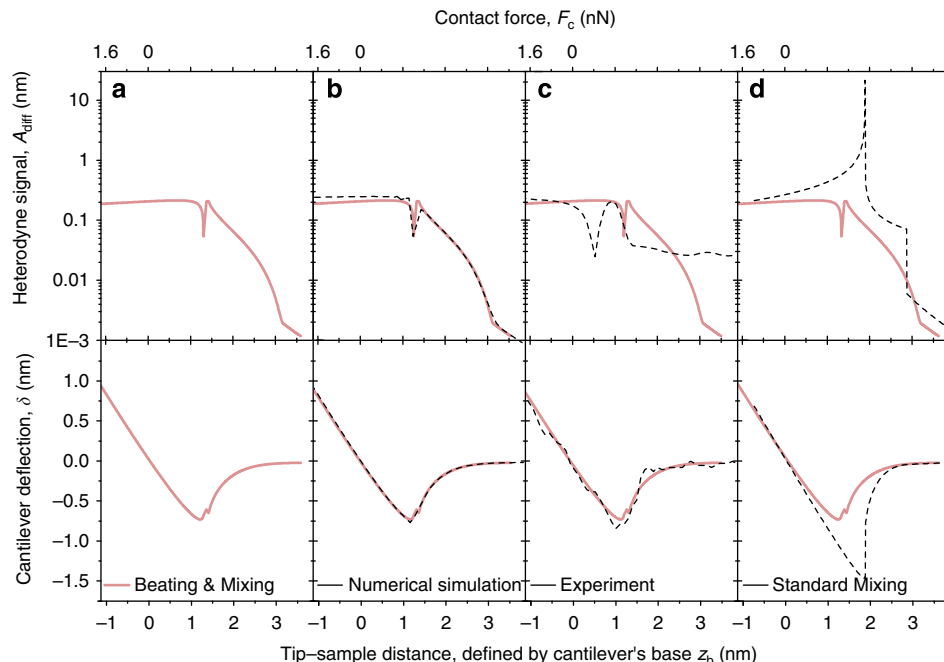


Figure 3 | Comparison between analytical theory, simulation, and an experiment. The heterodyne amplitude A_{diff} as obtained from ‘Beating & Mixing’ (a: red), from a full numerical simulation (b: black), from the experiment (c: black) and from ‘Standard Mixing’ (d: black). For comparison, the ‘Beating & Mixing’ curves (red) are also shown in b,c and d. The bottom panels show the corresponding static deflection δ of the cantilever. Notice that both the numerical simulation and the experimental results support the validity of ‘Beating & Mixing’: their curves qualitatively fit the ‘Beating & Mixing’ ones. In contrast, ‘Standard Mixing’ deviates significantly.

To confirm that ‘Beating & Mixing’ is important in HFM, we calculated both the amplitude of the heterodyne signal A_{diff} and the deflection δ as a function of the tip–sample distance (defined by the cantilever’s base position z_b ; see Fig. 3a). The numerical simulations quantitatively fit our ‘Beating & Mixing’ curves (see black line in Fig. 3b) perfectly. Additional proof comes also from experiments (see Fig. 3c)²¹, as the general curvature correctly reproduces the ‘Beating & Mixing’ results at all tip–sample distances z_b . If we compare the textbook solution of ‘Standard Mixing’ shown in Fig. 3d, one clearly notices a significant deviation: ‘Standard Mixing’ fails to describe the mixing signal. This is in contradiction with the general conception that standard frequency mixing generates the observed signal in HFM. The discontinuities, in both the amplitude and the deflection, are due to the specific choice of tip–sample interaction (see Supplementary Note 6). In conclusion, this confirms that ‘Beating & Mixing’ indeed correctly describes the generation the difference signal in HFM and that ‘Standard Mixing’ fails.

Discussion

Let us now discuss the significant effect of the ultrasound on the deflection in HFM, which can be evaluated by the static output (I_0) of the mixer with respect to the case without ultrasound. Alternatively, one can compare the deflection curves of the ‘Standard Mixing’ theory with the ‘Beating & Mixing’ theory, which is shown in Fig. 3d. In conclusion, both the adhesion and the elasticity appear smaller in HFM experiments, if one does not account for the existence of the ultrasound.

Finally, we address the more general case of heterodyne measurements without a back coupling to the input of the mixer as existent in HFM. Even without back coupling, beating is still essential to correctly describe the heterodyne signal generation. As the back coupling term in HFM is generated by I_1 (see Supplementary Note 4), we can set I_1 to zero in equation (2). Also without back coupling, ‘Beating & Mixing’ still determines the heterodyne signal and the static deflection through the parameters I_0 and I_2 . Therefore, we generally conclude that beating is of crucial importance for heterodyne detection schemes.

In conclusion, we have shown that beating, although it is a linear effect and has never considered to be of importance in heterodyne detection schemes, dominates the generation of the signal at the difference frequency in heterodyne measurements. We derived a general, analytical theory for any type of interaction that takes into account Beating & Mixing, and shown that our ‘Beating & Mixing’ theory correctly produces the standard beating solution for a pure linear interaction, as well as the Standard Mixing solution for an interaction that is purely quadratic. Correction terms are necessary for any interaction that is of higher order than quadratic. We verified our theory with a finite time step simulation and with an experiment applying HFM, which is a typical example of a heterodyne measurement with a highly non-quadratic mixer.

References

- Pfeifer, T. *et al.* Heterodyne mixing of laser fields for temporal gating of high-order harmonic generation. *Phys. Rev. Lett.* **97**, 163901 (2006).
- Berciaud, S., Cognet, L., Blab, G. A. & Lounis, B. Photothermal heterodyne imaging of individual nonfluorescent nanoclusters and nanocrystals. *Phys. Rev. Lett.* **93**, 257402 (2004).
- Turchette, Q. A., Hood, C. J., Lange, W., Mabuchi, H. & Kimble, H. J. Measurement of conditional phase shifts for quantum logic. *Phys. Rev. Lett.* **75**, 254710 (1995).
- Mlynek, J., Wong, N. C., DeVoe, R. G., Kintzer, E. S. & Brewer, R. G. Raman heterodyne detection of nuclear magnetic resonance. *Phys. Rev. Lett.* **50**, 130993 (1983).
- Diddams, S. A. *et al.* Direct link between microwave and optical frequencies with a 300 THz femtosecond laser comb. *Phys. Rev. Lett.* **84**, 225102 (2000).
- Matsuyama, E. *et al.* Principles and application of heterodyne scanning tunnelling spectroscopy. *Sci. Rep.* **4**, 6711 (2014).
- Thorne, K. S. Gravitational-wave research: current status and future prospects. *Rev. Mod. Phys.* **52**, 020285 (1980).
- Kolosov, O. & Yamanaka, K. Nonlinear detection of ultrasonic vibrations in an atomic force microscope. *Jpn J. Appl. Phys.* **32**, 8A11095 (1993).
- Yamanaka, K. & Nakano, S. Ultrasonic atomic force microscope with overtone excitation of cantilever. *Jpn J. Appl. Phys.* **35**, 6B3787 (1996).
- Cuberes, M. T., Assender, H. E., Briggs, G. A. D. & Kolosov, O. V. Heterodyne force microscopy of PMMA/rubber nanocomposites: nanomapping of viscoelastic response at ultrasonic frequencies. *J. Appl. Phys.* **D 33**, 192347 (2000).
- Shekhawat, G. S. & Dravid, V. P. Nanoscale imaging of buried structures via scanning near-field ultrasound holography. *Science* **310**, 574589 (2005).
- Cantrell, S. A., Cantrell, J. H. & Lillehei, P. T. Nanoscale subsurface imaging via resonant difference-frequency atomic force ultrasonic microscopy. *J. Appl. Phys.* **101**, 114324 (2007).
- Cuberes, M. T. Intermittent-contact heterodyne force microscopy. *J. Nanomater.* **2009**, 762016 (2009).
- Shekhawat, G. S., Srivastava, A., Avasthy, S. & Dravid, V. P. Ultrasound holography for noninvasive imaging of buried defects and interfaces for advanced interconnect architectures. *Appl. Phys. Lett.* **95**, 263101 (2009).
- Tetard, L. *et al.* Elastic phase response of silica nanoparticles buried in soft matter. *Appl. Phys. Lett.* **93**, 133113 (2008).
- Tetard, L. *et al.* Spectroscopy and atomic force microscopy of biomass. *Ultramicroscopy* **110**, 701–707 (2010).
- Tetard, L., Passian, A., Farahi, R. H. & Thundat, T. Atomic force microscopy of silica nanoparticles and carbon nanohorns in macrophages and red blood cells. *Ultramicroscopy* **110**, 586–591 (2010).
- Tetard, L., Passian, A. & Thundat, T. New modes for subsurface atomic force microscopy through nanomechanical coupling. *Nat. Nanotechnol.* **5**, 105–109 (2010).
- Tetard, L. *et al.* Imaging nanoparticles in cells by nanomechanical holography. *Nat. Nanotechnol.* **3**, 501–505 (2008).
- Verbiest, G. J., Oosterkamp, T. H. & Rost, M. J. Cantilever dynamics in heterodyne force microscopy. *Ultramicroscopy* **135**, 113–120 (2013).
- Verbiest, G. J., Oosterkamp, T. H. & Rost, M. J. Subsurface-AFM: sensitivity to the heterodyne signal. *Nanotechnology* **24**, 365701 (2013).
- Dejarguin, B. V., Muller, V. M. & Toporov, Y. P. Effect of contact deformations on the adhesion of particles. *J. Colloid Interf. Sci.* **53**, 314–326 (1975).

Acknowledgements

The research described in this paper has been performed under and financed by the NIMIC (<http://www.realnano.nl>) consortium under project 4.4. We acknowledge J.M. de Voogd, B. van Waarde and J.J.T. Wagenaar for proofreading of the manuscript.

Author contributions

M.J.R. realized the problem with beating. G.J.V. proposed the analytical model, worked out the equations and performed the experiments, as well as the simulations. Both authors discussed and interpreted the results, and also wrote the manuscript together. The project was initiated and conceptualized by M.J.R.

Additional information

Supplementary Information accompanies this paper at <http://www.nature.com/naturecommunications>

Competing financial interests: The authors declare no competing financial interest.

Reprints and permission information is available online at <http://npg.nature.com/reprintsandpermissions/>

How to cite this article: Verbiest, G. J. and Rost, M. J. Beating beats mixing in heterodyne detection schemes. *Nat. Commun.* 6:6444 doi: 10.1038/ncomms7444 (2015).